HHS Public Access

Author manuscript

J Neuroradiol. Author manuscript; available in PMC 2015 May 12.

Published in final edited form as:

J Neuroradiol. 2013 May ; 40(2): 81–88. doi:10.1016/j.neurad.2012.03.006.

Accuracy of head ultrasound for the detection of intracranial hemorrhage in preterm neonates: Comparison with brain MRI and susceptibility-weighted imaging

Jarunee Intrapiromkul[a], **Frances Northington**[c,d], **Thierry A.G.M. Huisman**[b,d], **Izlem Izbudak**[a,d], **Avner Meoded**[b], and **Aylin Tekes**[b,*,d]

[a]Divisions of Neuroradiology, Department of Radiology and Radiological Science, Johns Hopkins Hospital, Baltimore, MD 21287-0842, USA

[b]Division of Pediatric Radiology, Department of Radiology and Radiological Science, Johns Hopkins Hospital, 600, North Wolfe Street, Nelson Basement, B-172, Baltimore, MD 21287-0842, USA

[c]Division of Neonatology, Department of Pediatrics, Johns Hopkins Hospital, Baltimore, MD 21287-0842, USA

[d]Neurointensive Care Nursery, Johns Hopkins Hospital, Baltimore, MD 21287-0842, USA

Summary

Objectives—To evaluate the sensitivity and specificity of head ultrasound (HUS) in the detection of intracranial hemorrhage in premature neonates compared with brain MRI using susceptibility-weighted imaging (SWI).

Material and methods—Ultrasound (US) and MRI scans of the brain using SWI in premature neonates were retrospectively evaluated for grade I—III germinal matrix hemorrhage (GMH), periventricular hemorrhagic infarction (PVHI), intra-axial hemorrhage other than PVHI, extra-axial hemorrhage in each cerebral hemisphere and cerebellar hemorrhage in each cerebellar hemisphere. The impact of these hemorrhagic findings on short-term clinical management was also reviewed.

Results—Twelve neonates (mean age: 9.8 days; range: 3—23 days) with a mean gestational age of 32.8 weeks (range: 29.6—35.4 weeks) were included in the study. HUS had high sensitivity (100%) and specificity (93.3%) in detecting grade III GMH using SWI as a reference, but poor sensitivity (0%) in the detection of intraventricular hemorrhage with normal-sized ventricles (grade II GMH). US was not sensitive in detecting either small cerebellar or extra-axial hemorrhage.

Conclusion—HUS was highly sensitive and specific in the evaluation of grade III GMH, whereas SWI was superior to HUS in detecting small intra-axial or extra-axial hemorrhage, and

*Corresponding author. Tel.: +1 410 955 6454; fax: +1 410 502 3633. atekes1@jhmi.edu (A. Tekes).

Disclosure of interest

The authors declare that they have no conflicts of interest concerning this article.

had no impact on short-term management. Given the low cost, lack of radiation and advantages of bedside evaluation, HUS should continue to be the first line of imaging for brain injury in the evaluation of premature neonates with suspected intracranial hemorrhage. However, the usefulness of SWI for predicting long-term neurological outcomes has yet to be determined.

Keywords

Preterm; Hemorrhage; MRI; SWI; Ultrasound

Introduction

Intracranial hemorrhage (ICH) and white-matter injury are the major brain injuries that can occur in the developing brain of premature neonates. Germinal matrix hemorrhage (GMH), intraventricular hemorrhage (IVH), intraparenchymal hemorrhage and cerebellar hemorrhage have been recognized as the spectrum of ICH in premature infants. These brain injuries can have a significant impact on the morbidity, mortality and long-term neurodevelopment of premature infants [1,2]. For this reason, early and accurate diagnosis of ICH in premature infants is important, as appropriate management can minimize the sequelae to these injuries.

Head ultrasound (HUS), computed tomography (CT) and magnetic resonance imaging (MRI) have all been used to evaluate perinatal brain injury in premature infants. HUS is the current screening test for ICH in premature infants. As a portable imaging modality that is radiation-free, it is convenient and can safely be performed multiple times. Another advantage is its well-documented sensitivity in detecting ICH [3]. In addition, it enables acute imaging of these highly unstable infants and of the evolution of hemorrhage over time. MRI, however, is playing an ever-increasing role in perinatal brain injury, and has been reported to be superior to HUS in the evaluation of white-matter injury and ICH, especially in small quantities [3]. Furthermore, MRI can offer additional functional information through advanced MR techniques, such as diffusion tensor imaging (DTI) for the evaluation of white-matter maturation.

Susceptibility-weighted imaging (SWI) is an advanced MRI sequence that is being increasingly used in pediatric neuroimaging. It exploits the T2* properties of substances, which enhances the visualization of paramagnetic blood products (deoxyhemoglobin, intracellular methemoglobin and hemosiderin) [4]. SWI has been recognized to have greater sensitivity than conventional MRI sequences in detecting small hemorrhagic lesions [4-6]. SWI is also potentially useful in the evaluation of subtle white-matter abnormalities in infants by detecting small hemorrhages, postulated to be the potential etiology of punctate white-matter lesions of premature infants.

The aim of the present study was to determine the sensitivity of the current screening test for ICH in premature infants — HUS — and compare it with the most sensitive MR sequence for hemorrhage detection — SWI. Also evaluated was whether there is any impact on acute clinical management for the hemorrhages missed on ultrasound (US), but seen on MRI with SWI. Furthermore, the findings of ICH as seen on other conventional MR sequences,

including apparent diffusion coefficient (ADC) mapping from DTI, were compared with those visualized on SWI.

Material and methods

Participants

The radiological database was reviewed from December 2008 to April 2010 to identify premature neonates who had undergone both HUS and MRI. Premature neonates born at gestational age less than 36 weeks with HUS and MRI with SWI sequences at a postnatal age of less or equal to 1 month were included in this retrospective study. The study was approved by the institutional research board and was compliant with the Health Insurance Portability and Accountability Act (HIPAA) of 1996.

Imaging parameters

HUS was performed by experienced pediatric sonographers using state-of-the-art equipment (Zonare Medical Systems, Mountain View, CA, USA). A standardized set of images was obtained through the anterior fontanelle in coronal and sagittal planes using curved- and linear-array transducers (8—17 MHz). The angle of the transducer was varied when necessary to evaluate the brain periphery. Penetration depth, number of US foci, US gain and tissue brightness were optimized for each individual examination.

All neonates were scanned on a 1.5-Tesla MAGNETOM Avanto (Siemens AG, Erlangen, Germany). MRI sequences included T1- and T2-weighted images, fluid-attenuated inversion recovery (FLAIR), DTI and SWI. SWI used a strongly susceptibility-weighted low-bandwidth (80 Hz/pixel) 3D fast low-angle-shot sequence, with first-order flow compensation in all three orthogonal directions. The parameters for SWI were: TE/TR, 40/48 ms; flip angle, 15°; section thickness, 1.2 mm; FOV, 200 × 162; and matrix size 256 × 217. Acquisition time for each MRI sequence was: T1-weighted, 3.38 min; T2-weighted, 3.12 min; FLAIR, 3.2 min; DTI, 6.24 min; and SWI, 2.21 min.

Image analysis

The HUS and brain MRI—SWI scans were reviewed by two neuroradiologists, who evaluated the images on the picture archiving and communication system (PACS) by consensus. Both readers were qualified in reading HUS and MRI scans. HUS and brain MRI—SWI were evaluated 15 days apart, with the readers blinded to each other's results. HUS and brain MRI—SWI were evaluated in each hemisphere for the following findings: grade I, II and III GMH according to Papile's classification [7]; periventricular hemorrhagic infarction (PVHI) secondary to venous infarction (previously known as grade IV hemorrhage); intra-axial hemorrhage other than PVHI; extra-axial hemorrhage; and cerebellar hemorrhage. The grading of GMH was tabulated according to the highest degree of hemorrhage in that hemisphere: for example, a premature neonate with grade III hemorrhage was assigned to grade III hemorrhage only, with grades I and II considered 0. The DTI scans were interpreted according to signal alterations on ADC maps for detection of hemorrhage, and minimum-intensity-projection (mIP) data were used to evaluate hemorrhage on SWI. In premature infants at the correct location and clinical setting, it was

assumed that signal drops represented hemorrhage. However, given the lack of phase-contrast and magnitude images in our patients, it was not possible to further evaluate the images to differentiate hemorrhage from calcifications.

The data were analyzed using SPSS statistical software version 18. The ability of US to detect ICH compared with SWI was assessed in terms of sensitivity and specificity, using SWI as the gold standard. In addition, the patients' clinical charts were reviewed for treatment of ICH within 3 months of the latest imaging studies.

Results

Forty-three premature neonates who underwent MRI scans with SWI sequences were identified in the radiological database. Twenty-one cases were excluded due to age greater than 1 month at the time of MRI. Thus, 12 neonates (24 hemispheres) were included in our study. Those neonates were born at gestational age 32.8 ± 2 weeks (mean ± SD). US was performed at 7 ± 6.1 days postnatally (corrected post-conceptual age: 33.8 ± 2.5 weeks), and MRI was done within an interval of 2.7 ± 3.4 days.

Germinal matrix—intraventricular hemorrhages

Our study results are summarized in Table 1, while the sensitivity and specificity of HUS, conventional MR sequences and DTI in the detection of grade II GMH, grade III GMH and PVHI compared with SWI were shown in Table 2. In the present study, there was no infant with grade I GMH detected on SWI. However, two hemispheres were identified as grade I GMH on US (2/24, 8.3%), but were classified as grade II GMH using SWI, as GMH at the caudothalamic grooves and small IVH were depicted on SWI. Thus, the sensitivity and specificity in detecting grade I GMH could not be evaluated due to the absence of grade I GMH identified on SWI.

Grade II GMH was the most common GMH detected on SWI (87.5%, 21/24; Fig. 1), whereas it was noted on US in 33.3% (8/24). As for detection of grade II GMH using HUS, conventional MRI and DTI, HUS had the lowest sensitivity (0%, 0/10), while T2-weighted images (T2WI) had the highest sensitivity (100%, 10/10). Excellent specificity (100%) in detecting grade II GMH was noted with all modalities.

Out of all 24 hemispheres, grade III GMH was depicted on SWI in nine hemispheres (37.5%) and on US in 10 hemispheres (41.7%). Grade III GMH was also readily detected with all modalities (100% sensitivity and 93—100% specificity).

Periventricular hemorrhagic infarction

PVHI was depicted on SWI in 3/24 hemispheres (12.5%). All lesions were unilateral (left cerebral hemisphere in the frontal periventricular white-matter), and all imaging modalities (HUS, conventional MRI and DTI) were highly specific in the detection of PVHI (100%, 21/21). However, HUS was shown to be less sensitive than conventional MRI and DTI (66.7% *vs* 100% sensitivity, respectively) in PVHI detection.

Intracerebral hemorrhages (other than PVHI) were found on SWI in two hemispheres (8.3%). HUS and T2WI were able to detect the lesions in one of the two cases (50% sensitivity), whereas other MR sequences revealed both hemorrhages (100% sensitivity, 2/2). Fig. 2 shows the case in which T2WI failed to detect the intra-axial hemorrhage. Excellent specificity (100%, 22/22) of US and all MR sequences in the detection of ICH was also noted.

Extra-axial hemorrhage

US showed poor sensitivity in the detection of extra-axial hemorrhage in our study (10.5% sensitivity, 2/19). All of the extra-axial hemorrhages detected by US were large (two lesions, 1.6 ± 0.5 cm in width). In contrast, T1WI and T2WI (89.5% sensitivity, 17/19) and FLAIR sequences (73.7% sensitivity, 14/19) were sensitive and highly specific (100% specificity [5/5] for T1WI, T2WI and FLAIR) in the detection of extra-axial hemorrhage. However, DTI—ADC was less sensitive (47.4% sensitivity, 9/19) than conventional MR sequences in the detection of extra-axial hemorrhage.

Cerebellar hemorrhage

Cerebellar hemorrhages were detected on SWI in 20.8% of all hemispheres (5/24), and were punctate hemorrhages less than 3 mm at their greatest dimension (Fig. 3). None of these lesions was detected on either HUS or DTI—ADC. For the conventional MR sequences, cerebellar hemorrhages were best demonstrated on T1WI (80% sensitivity, 4/5; 100% specificity, 19/19), followed by T2WI (40% sensitivity, 2/5; 100% specificity, 19/19) and FLAIR (20% sensitivity, 1/5; 100% specificity, 19/19) sequences.

Review of the electronic patient records showed that one infant with a large subdural hematoma had undergone subgaleal shunt placement. The rest of the neonates with extra-axial hemorrhages (9/10 cases, 90%) required no surgical intervention. In all of the neonates with cerebellar hemorrhages (4/12 neonates, 33.3%), no intervention was performed for the punctate hemorrhages.

Discussion

Premature infants have an increased risk of long-term disability and early death compared with infants born at term. In the United States, infants born with a very low-birth-weight account for 1.5% of all live births and, of these, 50 to 70% survive. Of the survivors, 5 to 10% have major motor deficits (cerebral palsy), and 25 to 50% subsequently develop cognitive and behavioral deficits [8,9]. Hemodynamic alterations in premature infants can lead to various types of brain injury, predominantly GMH—IVH and periventricular white-matter injury.

GMH—IVH is the most common type of cerebral hemorrhage in premature infants, with an incidence of 15 to 25% [1]. Its mechanism is speculated to be multifactorial, involving vessel fragility and hemodynamic instability [1,10]. The severity grading of GMH—IVH was originally described by Papile et al. [7] in 1978, and was based on CT in very low-birth-weight infants: grade I hemorrhage was subependymal hemorrhage; grade II was IVH with no ventricular dilatation; grade III was IVH with ventricular dilatation; and grade IV was

IVH with parenchymal hemorrhage. Grade IV hemorrhage is known to result from venous infarction of the intramedullary veins because of impaired venous drainage caused by compression due to GMH to IVH. Venous infarction is generally followed by hemorrhagic conversion, hence the term ‘‘periventricular hemorrhagic infarction’’ (PVHI) [1,11,12]. In general, 40% of cases of GMH—IVH have an onset within 5 hours of birth and 90% arise within the first 4 days [11]. At present, US is the routine screening test for GMH—IVH and other brain injury in preterm infants.

In our present study, no neonate with grade I GMH was recruited, which made it impossible to assess the sensitivity and specificity of detecting grade I GMH. However, it is likely that the mild injury of grade I GMH and its more benign clinical course would elicit no indication for an MRI study. Yet, based on our present observations, GMH can easily be visualized by HUS as a hyperechoic focus at the caudothalamic notch (Fig. 4). However, our study has demonstrated that HUS had poor sensitivity in detecting grade II GMH. The blood-filled ventricle appears hyperechoic on HUS, which may sometimes be difficult to differentiate from hyperechoic choroid plexus. Small amounts of IVH may be localized in the occipital horn of the lateral ventricle, the most dependent part in the supine position, but were suboptimally assessed by HUS using the anterior fontanelle approach.

In fact, our study found that small IVH were better visualized by SWI. In cases with tiny amounts of IVH, the linear hypointensity of hemosiderin lining the ventricle can be seen on SWI, making this the most sensitive method for detecting grade II GMH. Also, in our study, there were two grade II GMH lesions that were misdiagnosed as grade I GMH on US. In these cases, SWI was able to identify GMH at the caudothalamic groove as well as the small IVH. However, due to the poorer sensitivity of US in the detection of small IVH, the technology failed to detect small IVH in these two cases, leading to undergrading of GMH. Nevertheless, IVH with a dilated ventricle was easily depicted on US, conventional MRI and SWI, which contributed to the excellent sensitivity and specificity of all modalities in detecting grade III GMH.

PVHI was once assumed to result from the extension of IVH into the brain parenchyma. Recently, however, it has been found to result from venous infarction and hemorrhagic conversion due to occlusion of the collector veins [13]. Both US and MRI can demonstrate early-stage PVHI as a fan-shaped periventricular lesion along the distribution of medullary veins (Fig. 5) [10,14]. Our present study demonstrated that HUS was highly sensitive in identifying extensive PVHI, but not small focal PVHI (Fig. 6). In contrast, in all cases with PVHI, SWI revealed the characteristic finding of linear hypointensities following the medullary venous distribution. These hypointense lines could correspond to the perivascular hemorrhages found along medullary veins in a previous histopathological study [15].

Our present finding of the poor sensitivity of HUS in the detection of small cerebellar hemorrhages (Fig. 3) and small extra-axial hemorrhages (Fig. 1C and D) could be explained by the greater spatial resolution and contrast of MRI in the visualization of small hemorrhages. Although short-term management is not required for small cerebellar and small extra-axial hemorrhages, such small cerebellar hemorrhages solely detected on MRI

were found in a recent study to be associated with an increased risk of neurological deficit [16].

The lack of long-term neurological outcome data is one of the limitations of our present retrospective study. Thus, further studies of a large number of premature neonates with various types of ICH as detected by SWI, and correlated with their long-term neurological outcomes, might establish the role of SWI as a better long-term outcome predictor. If the clinical impact of small hemorrhages as solely detected on SWI were to be well established, it would then be worthwhile to screen every preterm neonate with SWI for microhemorrhages. However, without pathological proof, we chose to use SWI as the gold standard, thus prohibiting direct comparisons of accuracy between modalities.

In the present study, only premature neonates who had undergone brain MRI with SWI and HUS imaging studies were recruited, which might raise the possibility of selection bias, as not all premature neonates had MRI scans. Indeed, in our practice, only neonates with questionable severe brain injury or abnormality are sent for MRI, which also explains the absence of grade I GMH in our study.

HUS using only the anterior fontanelle approach is another limitation of our study. Previous publications have shown that posterior fontanelle and mastoid fontanelle imaging techniques are useful for the detection of posterior fossa abnormalities and small IVH with normal-sized ventricles [17-19]. Indeed, additional US windows may have increased the sensitivity of US in the detection of posterior fossa hemorrhage as well as grade II hemorrhage in our present study. Also, US image quality is recognized to be operator-dependent and, although our sonographers are well trained for US in pediatric patients, there are still variations in skill among operators.

Our present study has suggested the advantages of including SWI in the neonatal brain MRI protocol. Hemorrhagic brain injury is frequently seen in premature neonates and, given that SWI has a high sensitivity to detect hemorrhage, SWI could be an excellent tool for identifying those brain injuries in premature neonates that may not be apparent on conventional MRI sequences. Moreover, in conjunction with conventional MRI sequences, SWI can provide additional information on other neurological disorders that can arise in neonates, such as traumatic brain injury, vascular malformation, infarction, neoplasm and venous thrombosis.

Conclusion

SWI is a valuable sequence for brain imaging in premature neonates and should be included as part of the neonatal brain MRI protocol. It is highly sensitive in detecting ICH and can also provide information on its full extent. HUS has proven to have good sensitivity in the detection of grade I and III GMH, and is adequate for diagnosing cases that require short-term surgical management due to complications of IVH. Also, as HUS is the least-invasive imaging modality and can be performed at bedside, it is the most suitable screening test for ICH in preterm neonates. Nevertheless, the usefulness of SWI in predicting long-term neurological outcomes has still to be determined.

References

1. Bassan H. Intracranial hemorrhage in the preterm infant: understanding it, preventing it. Clin Perinatol. 2009; 36:737–62. v. [PubMed: 19944833]
2. Rutherford MA, Supramaniam V, Ederies A, Chew A, Bassi L, Groppo M, et al. Magnetic resonance imaging of white-matter diseases of prematurity. Neuroradiology. 2010; 52:505–21. [PubMed: 20422407]
3. Maalouf EF, Duggan PJ, Counsell SJ, Rutherford MA, Cowan F, Azzopardi D, et al. Comparison of findings on cranial ultrasound and magnetic resonance imaging in preterm infants. Pediatrics. 2001; 107:719–27. [PubMed: 11335750]
4. Tong KA, Ashwal S, Obenaus A, Nickerson JP, Kido D, Haacke EM, et al. imaging: a review of clinical applications in children. AJNR Am J Neuroradiol. 2008; 29:9–17. [PubMed: 17925363]
5. de Souza JM, Domingues RC, Cruz LC Jr, Domingues FS, Ias-beck T, Gasparetto EL. Susceptibility-weighted imaging for the evaluation of patients with familial cerebral cavernous malformations: a comparison with t2-weighted fast spinecho and gradient-echo sequences. AJNR Am J Neuroradiol. 2008; 29:154–8. [PubMed: 17947370]
6. Nandigam RN, Viswanathan A, Delgado P, Skehan ME, Smith EE, Rosand J, et al. MR imaging detection of cerebral microbleeds: effect of susceptibility-weighted imaging, section thickness, and field strength. AJNR Am J Neuroradiol. 2009; 30:338–43. [PubMed: 19001544]
7. Papile LA, Burstein J, Burstein R, Koffler H. Incidence and evolution of subependymal and intraventricular hemorrhage: a study of infants with birth weights less than 1,500 gm. J Pediatr. 1978; 92:529–34. [PubMed: 305471]
8. Volpe JJ. Brain injury in premature infants: a complex amalgam of destructive and developmental disturbances. Lancet Neurol. 2009; 8:110–24. [PubMed: 19081519]
9. Kinney HC. The near-term (late preterm) human brain and risk for periventricular leukomalacia: a review. Semin Perinatol. 2006; 30:81–8. [PubMed: 16731282]
10. Argyropoulou MI. Brain lesions in preterm infants: initial diagnosis and follow-up. Pediatr Radiol. 2010; 40:811–8. [PubMed: 20431999]
11. Barkovich, AJ. Pediatric neuroimaging. Philadelphia: Lippincott Williams & Wilkins; 2005. p. 209-215.
12. Volpe JJ. Brain injury in the premature infant: overview of clinical aspects, neuropathology, and pathogenesis. Semin Pediatr Neurol. 1998; 5:135–51. [PubMed: 9777673]
13. Dudink J, Lequin M, Weisglas-Kuperus N, Conneman N, van Goudoever JB, Govaert P. Venous subtypes of preterm periventricular haemorrhagic infarction. Arch Dis Child Fetal Neonatal Ed. 2008; 93:F201–6. [PubMed: 17768152]
14. de Vries LS, Roelants-van Rijn AM, Rademaker KJ, Van Haastert IC, Beek FJ, Groenendaal F. Unilateral parenchymal haemorrhagic infarction in the preterm infant. Eur J Paediatr Neurol. 2001; 5:139–49. [PubMed: 11587377]
15. Gould SJ, Howard S, Hope PL, Reynolds EO. Periventricular intraparenchymal cerebral haemorrhage in preterm infants: the role of venous infarction. J Pathol. 1987; 151:197–202. [PubMed: 3572613]
16. Tam EW, Rosenbluth G, Rogers EE, Ferriero DM, Glidden D, Goldstein RB, et al. Cerebellar hemorrhage on magnetic resonance imaging in preterm newborns associated with abnormal neurologic outcome. J Pediatr. 2010; 158:245–50. [PubMed: 20833401]
17. Di Salvo DN. A new view of the neonatal brain: clinical utility of supplemental neurologic US imaging windows. Radiographics. 2001; 21:943–55. [PubMed: 11452069]
18. Anderson N, Allan R, Darlow B, Malpas T. Diagnosis of intraventricular hemorrhage in the newborn: value of sonography via the posterior fontanelle. AJR Am J Roentgenol. 1994; 163:893–6. [PubMed: 8092030]
19. Correa F, Enriquez G, Rossello J, Lucaya J, Piqueras J, Aso C, et al. Posterior fontanelle sonography: an acoustic window into the neonatal brain. AJNR Am J Neuroradiol. 2004; 25:1274–82. [PubMed: 15313724]

Abbreviations

ADC	Apparent diffusion coefficient
CT	Computed tomography
DTI	Diffusion tensor imaging
FLAIR	Fluid-attenuated inversion recovery
GMH	Germinal matrix hemorrhage
HUS	Head ultrasound
ICH	Intracranial hemorrhage
IVH	Intraventricular hemorrhage
MRI	Magnetic resonance imaging
PVHI	Periventricular hemorrhagic infarction
SWI	Susceptibility-weighted imaging
T1WI	T1-weighted images
T2WI	T2-weighted images

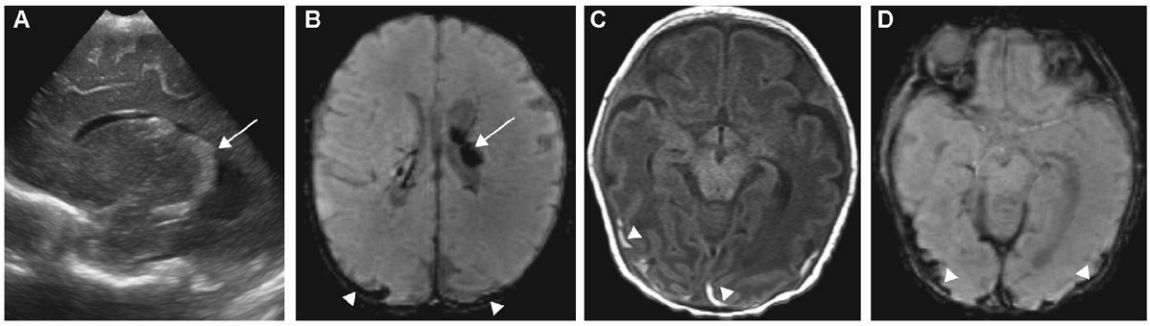

Figure 1.

Grade II germinal matrix hemorrhage (GMH): (A) left sagittal ultrasound (US) image shows hyperechoic enlarged choroid plexus (arrow); (B) axial minimum-intensity-projection (mIP) susceptibility-weighted imaging (SWI) shows dark signal intensity of choroid plexus within the left lateral ventricle compatible with grade II GMH (arrow); (C) thin subdural hematoma along bilateral occipital convexities seen on axial T1-weighted images (T1WI); and on (D) axial mIP SWI (arrowheads), but missed on US.

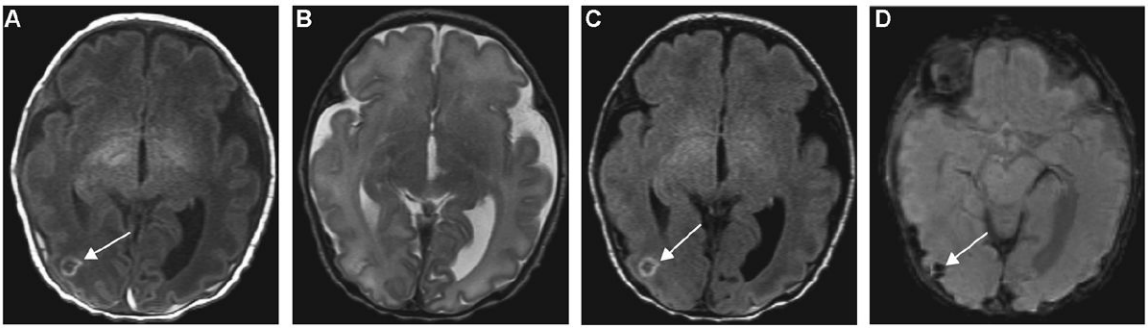

Figure 2.

A 6-day-old ex-34-week male neonate with intra-axial hemorrhage: (A) axial T1-weighted (T1W) and (C) fluid-attenuated inversion recovery (FLAIR) images show a small rounded isointense lesion with peripheral hyperintensity in the right occipital region (arrows), corresponding to (D) the dark signal intensity on susceptibility-weighted imaging (SWI) (arrow). This lesion was not visualized on the T2W image (B), although hemorrhage is expected to be better depicted by T2WI than other conventional magnetic resonance imaging (MRI) sequences.

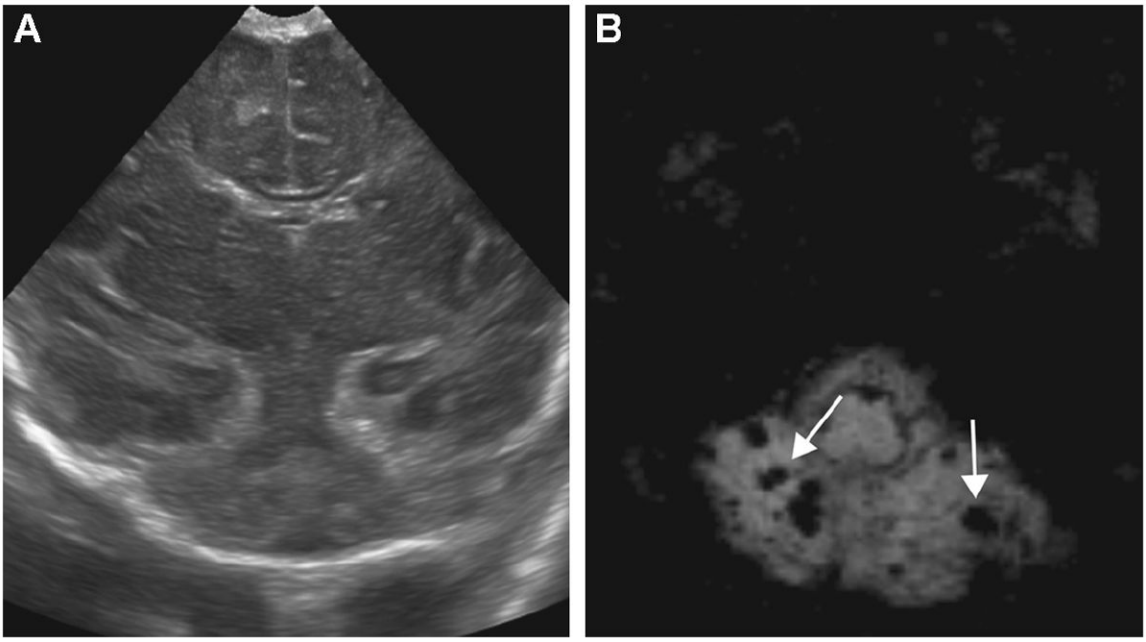

Figure 3.

A 5-day-old ex-34-week male neonate with perinatal depression: (B) axial susceptibility-weighted imaging (SWI) shows multiple microbleeds in the cerebellum (arrows) that were undetectable by ultrasound (US) (A).

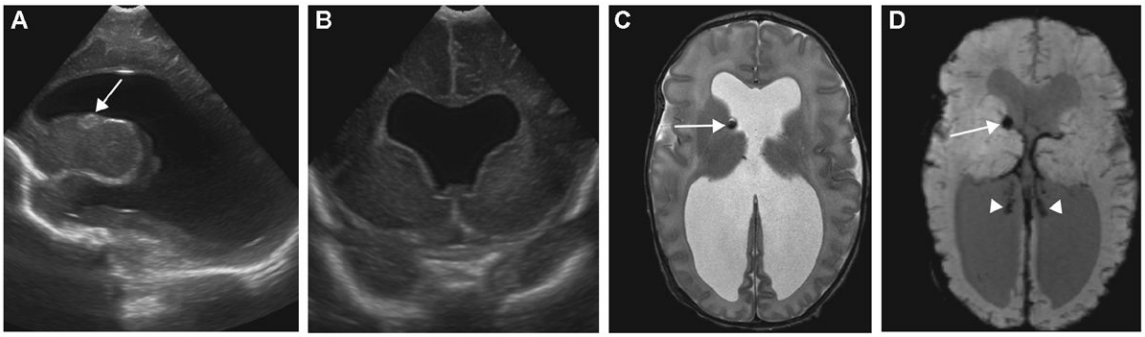

Figure 4.

A 20-day-old ex-35-week twin with grade III germinal matrix hemorrhage (GMH) and septo-optic dysplasia: (A) right sagittal ultrasound (US) image, (B) coronal US image, and (D) axial T2WI and axial minimal-intensity-projection (mIP) susceptibility-weighted imaging (SWI) show dilated ventricles. GMH at the right caudothalamic groove is depicted on (A) US, (C) T2WI and (D) SWI (arrows). Dark signal intensity of choroid plexus on SWI (D) represents hemorrhage overlying the choroid plexus (arrowheads). (B–D) Absence of septum pellucidum is also evident.

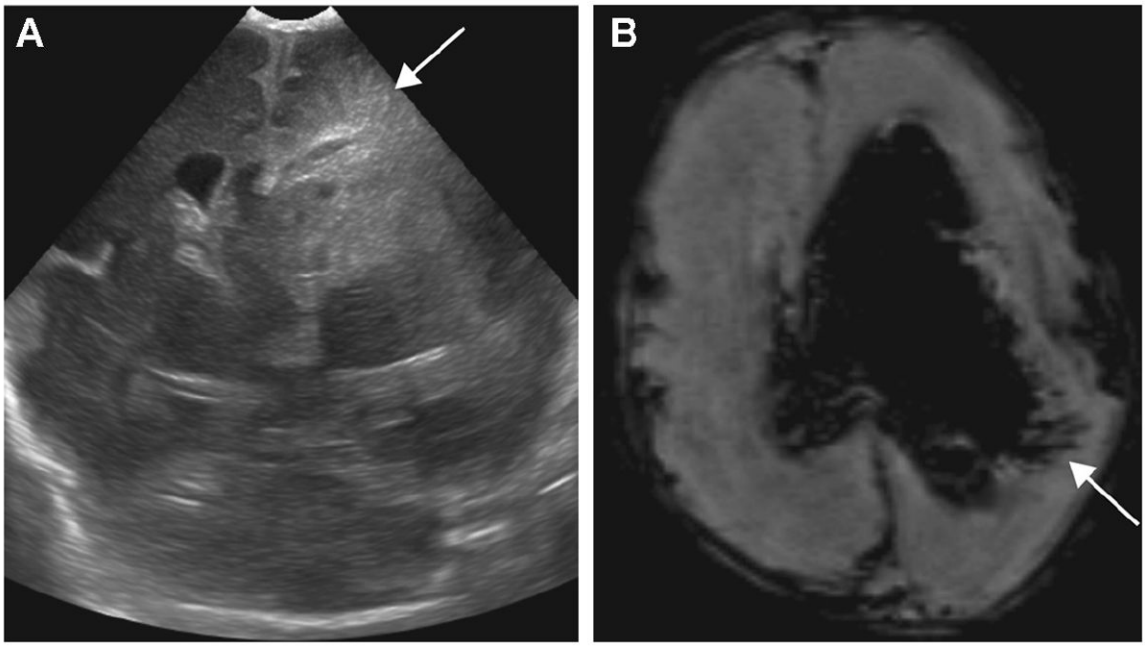

Figure 5.

A 23-day-old ex-30-week male neonate with periventricular hemorrhagic infarction (PVHI): (A) coronal ultrasound (US) image shows triangular (fan-shaped) echodensities radiating from the left lateral ventricle (arrow). The linear dark signal intensities leading from the lateral ventricle in association with intraventricular hemorrhage (IVH) are well demonstrated on (B) axial susceptibility-weighted imaging (SWI) (arrow).

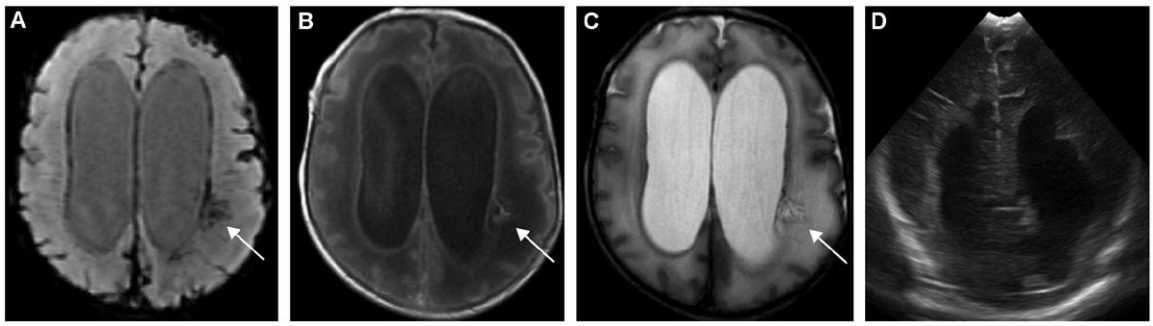

Figure 6.

An 18-day-old ex-33-week male neonate with intraventricular hemorrhage (IVH), hydrocephalus and periventricular hemorrhagic infarction (PVHI): (A) axial susceptibility-weighted imaging (SWI) shows a focal area of linear hypointensities radiating from the left lateral ventricle in the periventricular white-matter, which corresponds to the focal hyperintensity on (B) axial T1-weighted images (T1WI) and (C) hypointensity on T2WI (arrows), demonstrating venous ischemia with hemorrhage. However, this lesion is not visualized on (D) ultrasound (US). The linear dark signal intensity lining the ventricle (A), representing IVH as seen on SWI, was again not apparent on US.

Table 1

Number of brain hemispheres with intracranial hemorrhages as detected by susceptibility-weighted imaging (SWI), ultrasound (US), conventional magnetic resonance imaging (MRI) and diffusion tensor imaging (DTI).

	Grade I GMH	Grade II GMH	Grade III GMH	PVHI	Other intracerebral hemorrhage	Extra-axial hemorrhage	Cerebellar hemorrhage
SWI	0/24 (0%)	10/24 (41.7%)	9/24 (37.5%)	3/24 (12.5%)	2/24 (8.3%)	19/24 (79.2%)	5/24 (20.8%)
MRI							
T1WI	0/24 (0%)	5/24 (20.8%)	9/24 (37.5%)	3/24 (12.5%)	2/24 (8.3%)	17/24 (70.8%)	4/24 (16.7%)
T2WI	0/24 (0%)	10/24 (41.7%)	9/24 (37.5%)	3/24 (12.5%)	1/24 (4.2%)	17/24 (70.8%)	2/24 (8.3%)
FLAIR	0/24 (0%)	1/24 (4.2%)	9/24 (37.5%)	3/24 (12.5%)	2/24 (8.3%)	14/24 (58.3%)	1/24 (4.2%)
DTI—ADC	0/24 (0%)	3/24 (12.5%)	9/24 (37.5%)	3/24 (12.5%)	2/24 (8.3%)	9/24 (37.5%)	0/24 (0%)
US	2/24 (8.3%)	0/24 (0%)	10/24 (41.7%)	2/24 (8.3%)	1/24 (4.2%)	2/24 (8.3%)	0/24 (0%)

GMH: germinal matrix hemorrhage; PVHI: periventricular hemorrhagic infarction; SWI: susceptibility-weighted imaging; MRI: magnetic resonance imaging; T1/T2WI: T1-weighted/T2-weighted imaging; FLAIR: fluid-attenuated inversion recovery; DTI: diffusion tensor imaging; ADC: apparent diffusion coefficient; US: ultrasound.

Table 2

Sensitivity and specificity of ultrasound (US) and conventional magnetic resonance imaging (MRI) in the detection of germinal matrix hemorrhage (GMH) and periventricular hemorrhagic infarction (PVHI) *vs* susceptibility-weighted imaging (SWI).

	Grade II GMH		Grade III GMH		PVHI	
	Sensitivity	**Specificity**	**Sensitivity**	**Specificity**	**Sensitivity**	**Specificity**
US	0% (0/10)	100% (14/14)	100% (9/9)	93.3% (14/15)	66.7% (2/3)	100% (21/21)
T1WI	50% (5/10)	100% (14/14)	100% (9/9)	100% (15/15)	100% (3/3)	100% (21/21)
T2WI	100% (10/10)	100% (14/14)	100% (9/9)	100% (15/15)	100% (3/3)	100% (21/21)
FLAIR	10% (1/10)	100% (14/14)	100% (9/9)	100% (15/15)	100% (3/3)	100% (21/21)
DTI—ADC	30% (3/10)	100% (14/14)	100% (9/9)	100% (15/15)	100% (3/3)	100% (21/21)

US: ultrasound; MRI: magnetic resonance imaging; GMH: germinal matrix hemorrhage; PVHI: periventricular hemorrhagic infarction; SWI: susceptibility-weighted imaging; T1/T2WI: T1-weighted/T2-weighted imaging; FLAIR: fluid-attenuated inversion recovery; DTI: diffusion tensor imaging; ADC: apparent diffusion coefficient.